IET Communications

Research Article

IET Journals
The Institution of Engineering and Technology

Achievable rates and outage probability of cognitive radio with dynamic frequency hopping under imperfect spectrum sensing

ISSN 1751-8628
Received on 25th January 2015
Revised on 4th August 2015
Accepted on 14th August 2015
doi: 10.1049/iet-com.2015.0094
www.ietdl.org

Anh D. Le[1] ✉, *Sanjeewa P. Herath*[2], *Nghi H. Tran*[1], *Trung Q. Duong*[3,4], *Sachin Shetty*[5]

[1]*Department of Electrical and Computer Engineering, University of Akron, Akron, USA*
[2]*Department of Electrical and Computer Engineering, McGill University, Room 633, McConnell Engineering Building 3480 University Street, Montreal, Canada H3A 0E9*
[3]*School of Electronics, Electrical Engineering and Computer Science, Queen's University of Belfast, Belfast, UK*
[4]*Duy Tan University, Da Nang, Vietnam*
[5]*Department of Electrical and Computer Engineering Department, Tennessee State University, Nashville, USA*
✉ *E-mail: adl47@zips.uakron.edu*

Abstract: In this study, the authors propose simple methods to evaluate the achievable rates and outage probability of a cognitive radio (CR) link that takes into account the imperfectness of spectrum sensing. In the considered system, the CR transmitter and receiver correlatively sense and dynamically exploit the spectrum pool via dynamic frequency hopping. Under imperfect spectrum sensing, false-alarm and miss-detection occur which cause impulsive interference emerged from collisions due to the simultaneous spectrum access of primary and cognitive users. That makes it very challenging to evaluate the achievable rates. By first examining the static link where the channel is assumed to be constant over time, they show that the achievable rate using a Gaussian input can be calculated accurately through a simple series representation. In the second part of this study, they extend the calculation of the achievable rate to wireless fading environments. To take into account the effect of fading, they introduce a piece-wise linear curve fitting-based method to approximate the instantaneous achievable rate curve as a combination of linear segments. It is then demonstrated that the ergodic achievable rate in fast fading and the outage probability in slow fading can be calculated to achieve any given accuracy level.

1 Introduction

This work was partially supported by the National Science Foundation, USA, under Grant No. 1509006. A part of this work was presented at the IEEE Int. Conf. on Commun. and Electronics (ICCE), Da Nang. August 2014 [1]. Cognitive radio (CR) has been considered as a revolutionary wireless communication paradigm [2] to improve the spectral efficiency. In CR, unlicenced users, or secondary users (SUs), are allowed to access the frequency bands (F-bands) when primary users (PUs) are absent [2]. By intelligently sensing and adapting to the environment, SUs can identify the temporal communications opportunities (spectrum holes) and utilise them without causing harmful interference to PUs' communication links. One of the prospective CR models is dynamic frequency hopping (DFH) [3, 4] in which the working F-bands of PUs users are divided into small sub-channels to form a spectrum pool. An SU can exploit this spectrum pool by performing spectrum sensing and dynamically hopping over these sub-channels to establish SU communication links when temporal white spaces are available. In fact, this set of sub-channels is dynamically changed depending on PU activities over the channel. Once PU wants its own resources, all SUs must leave, releasing the corresponding vacant sub-channels to the PU [3]. Since SUs dynamically hop over sub-channels, their links are less affected by PU activities [5].

While spectrum sensing can be performed effectively using various advanced sensing schemes (please see [6, 7] and references therein), this operation is not perfect in practice, which results in false-alarm and miss-detection events. When we have false-alarm, the SU fails to utilise the interference-free channel. On the other hand, when the miss-detection happens, an SU fails to detect an active PU and collisions occur. As a result, impulsive interference is generated due to the simultaneous spectrum access of both PU and SU and affects the CR link. While considering the imperfectness of spectrum sensing at the CR transmitter (TX), the analysis in [8, 9] studied the achievable rate under the assumption of perfect knowledge of the state of the PU interference at the CR receiver (RX). Therefore, the achievable rate can only be considered as an upper-bound on the capacity of a CR link. Some recent efforts have studied cooperative sensing techniques [10, 11] and intelligent power control [12, 13] to enhance the CR performance. However, these works do not completely take into account the miss-detection and false-alarm events. The sensing-energy efficiency and sensing-throughput trade-off of CR networks have also been investigated in [9, 14] but with the same drawbacks. Recently, the error performance of CR systems has been analysed under imperfect spectrum sensing in [15] but the results apply to only uncoded CR systems. In a practical scenario under miss-detection and false-alarm events, due to the presence of interference generated from the PU, the channel is no longer Gaussian and calculating the achievable rate is very difficult. Herath *et al.* in [16] attempted to study the achievable rate of such a CR link using DFH in a frequency pool for opportunistic spectrum sharing. Under the assumption that both the CR TX and RX can access the same sensing information, the achievable rates are calculated based on raw approximations. As a consequence, the accuracy level cannot be controlled. In addition, the work in [16] assumed a static CR channel where the channel gains are assumed to be constant. This assumption therefore does not fit very well to a dynamic fading wireless environment. The raw calculations in [16] cannot be extended to such circumstance, since one needs to consider the effects of fading in addition to impulsive interference from PUs.

Motivated by the above observation, in this paper, we propose a simple method to accurately evaluate the achievable rate of a realistic CR link using DFH in a frequency pool for opportunistic

spectrum sharing that takes into account the imperfectness of spectrum sensing. While this work can be considered as an extension of our prior work in [16], the contributions of this submission are much more comprehensive where novel methods are proposed to calculate the achievable rates and the outage probabilities over both static and fading channels to achieve any accuracy level. Extensive Monte Carlo simulations are therefore no longer needed. Our detailed contributions can be summarised as follows:

- In the first part of this paper, we consider the static channel model where the channel gain remains constant as similar to [16]. However, instead of using raw approximations, we show that the information rate achieved by a Gaussian input can be calculated using a simple series representation. This provides an effective and accurate way to calculate the achievable rate.
- More importantly, we extend the calculation of the ergodic achievable rate in fast Rayleigh fading and the outage probability in slow Rayleigh fading environments in the second part of this paper. Given that the instantaneous achievable rate can be expressed in closed-form, we propose a piece-wise linear curve fitting (PLCF)-based method to approximate the instantaneous achievable rates curve as a combination of linear segments. It is then demonstrated that the ergodic achievable rate in fast fading and the outage probability in slow fading of the considered CR systems in the presence of sensing imperfection can be calculated effectively to achieve any given accuracy level.

The remainder of this paper is organised as follows. In Section 2, the considered DFH CR link is introduced. Section 3 presents a simple way to calculate the achievable rate over the static channel to achieve any predetermined accuracy level. In Section 4, the calculation of the ergodic achievable rate in fast fading environment is provided. The calculation of the outage probability in slow fading is also presented in this section. Numerical results are then provided in Section 5 to confirm the analysis. Finally, Section 6 concludes this paper.

2 CR under DFH: system model

2.1 Channel model

In this paper, we consider the CR system employing DFH as in [3, 15]. In this DFH system, the PU utilises an F-band in a time-slotted transmission structure and it is assumed that the PU occupies a time-slot with probability p. As shown in Fig. 1, a frequency spectrum pool is formed by using several frequency subchannels over PU F-bands [3, 4]. The SU then dynamically hops over these sub-channels and establishes its transmission when the channel is free of PU signal. We assume that the hopping sequence is known to both SU TX and RX [16, 17], and the SU is synchronised with the PU time-slot structure [18]. At the beginning of each time-slot, a decision regarding the presence or absence of PU signals is made available at both the SU TX and RX. This can be achieved when the RX knows the sensing information from the TX via a reliable feedforward link. In a more practical scenario, a fusion sensing architecture can be employed to collect all sensing information and a final sensing decision is made at an access point and sent to the SU terminals [19].

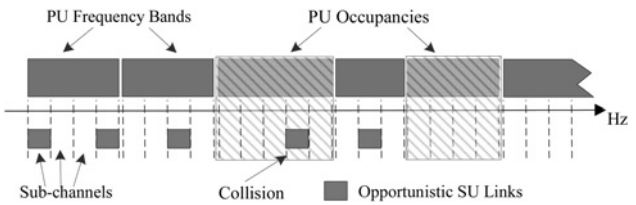

Fig. 1 *Frequency spectrum pool in PU F-bands*

Since the spectrum sensing is not perfect in practice, it is important to take into account the imperfectness of the spectrum sensing, which is characterised by the probabilities of miss-detection and false-alarm with the probabilities P_{m} and P_{f}, respectively [20]. Under the miss-detection event, SU fails to detect an active PU. In this event, the SU link is affected by an impulsive interference generated from the PU transmission. On the other hand, false-alarm occurs in the event that no PU is active but SU postulates one. Furthermore, in the events of false-alarm with probability P_{f} and correct detection with probability $(1-P_{\mathrm{m}})$, the SU channel outputs are respectively noise and noise plus interference only (i.e. without SU transmission). Depending on the sensing techniques applied, for example, energy detection [6], we can calculate these two parameters straightforwardly [21]. It is clear that P_{m} and P_{f} depend on the noise level, and the strength of interfering signal from PU.

To establish the channel model of interest in further detail, let b_e be a Bernoulli random variable that represents the cases of SU perceiving either a busy time-slot, that is, $\mathcal{P}(b_e=0)$, or free time-slot, that is, $\mathcal{P}(b_e=1)$. It can be seen that the event $b_e=0$ indicates the case of false-alarm or correct detection. Therefore, $\mathcal{P}(b_e=0)=p(1-P_{\mathrm{m}})+(1-p)P_{\mathrm{f}}$. Under this event, SU TX keeps silent and channel erasure can be declared by SU RX. On the other hand, under the event $b_e=1$, the channel is considered to be free from SU perspective and SU TX will transmit a complex signal $\boldsymbol{x}$. Taking into account the miss-detection event of the presence of a PU, the channel output $\boldsymbol{y}$ can then be expressed as

$$\boldsymbol{y}|_{b_e=1}=g\cdot\boldsymbol{x}+b_{\mathrm{m}}\boldsymbol{I}+\boldsymbol{n}. \tag{1}$$

In (1), b_{m} is Bernoulli random variables with state space $\{0,\ 1\}$ where '$b_{\mathrm{m}}=1$' indicates the miss-detection of the presence of a PU and we have $\mathcal{P}(b_{\mathrm{m}}=1)=pP_{\mathrm{m}}\triangleq p_1$. For convenience, we denote $p_e\triangleq\mathcal{P}(b_e=1)$ throughout this paper. Note that the input is subject to the average power constraint $\mathbb{E}(b_e|\boldsymbol{x}|^2)\le 2P_x$. Moreover in (1), g is the channel gain, $\boldsymbol{n}\sim\mathcal{CN}\left(0,\ 2\sigma_n^2\right)$ represents the thermal noise, and $\boldsymbol{I}$ is the PU interference seen by SU RX, $\boldsymbol{I}\sim\mathcal{CN}\left(0,\ 2\sigma_I^2\right)$. We also define $\boldsymbol{n}_{\mathrm{T}}\triangleq b_{\mathrm{m}}\boldsymbol{I}+\boldsymbol{n}$ as a total noise, which is no longer Gaussian distributed.

In this paper, we consider two different cases of the channel gain g. Specifically, for a static channel as in [16], we have $g=1$. On the other hand, in a wireless fading environment, we consider Rayleigh fading in which the magnitude of g follows Rayleigh distribution, or equivalently, $\alpha=|g|^2$ is exponentially distributed. It is also assumed that g is available at the CR RX but not the TX.

2.2 Achievable rates and outage probability

For the above model, as shown in [16], the use of a Gaussian input $\boldsymbol{x}$ is asymptotically optimal. As such, for a static channel with $g=1$, the information rate achieved by the Gaussian input can be calculated as

$$\begin{aligned}C_{\mathrm{s}}&=\mathcal{I}(\boldsymbol{x};\ \boldsymbol{y},\ b_e)=\mathcal{I}(\boldsymbol{x};\ b_e)+\mathcal{I}(\boldsymbol{x};\ y|b_e)\\&=\mathcal{P}(b_e=1)\mathcal{I}(\boldsymbol{x};\ y|b_e=1)\\&=p_e[h(\boldsymbol{y})-h(\boldsymbol{n}_{\mathrm{T}})]\end{aligned} \tag{2}$$

where $\mathcal{I}(\cdot)$ is the mutual information between the corresponding variables and $h(\boldsymbol{y})$ and $h(\boldsymbol{n}_{\mathrm{T}})$ are entropy values of $\boldsymbol{y}$ and $\boldsymbol{n}_{\mathrm{T}}$, respectively. It should be noted that the above achievable rate corresponds to the case of $b_e=1$. It is because the SU RX declares channel erasures on the noise and noise plus interference outputs when we have the realisation $b_e=0$.

In the case of fading channels and under the assumption of ergodicity for fading gains, g can be assumed to change independently from symbol to symbol. Therefore, the ergodic achievable rate can be obtained by averaging over the fading gain g as follows

$$C_{\mathrm{f}}=p_e[\mathbb{E}_g[h(\boldsymbol{y}|g)]-h(\boldsymbol{n}_{\mathrm{T}})]. \tag{3}$$

In (3), $h(\boldsymbol{y}|g)$ is the differential entropy of the output for a given g. On the other hand, for a slow fading channel where g is assumed to remain constant, one has the outage probability, which is defined as the probability that the achievable rate for a given realisation g is smaller than a desired rate r. The outage probability can be expressed as

$$P_{\text{out}}(r) = \Pr\{[h(\boldsymbol{y}|g) - h(\boldsymbol{n}_{\text{T}})] \leq r\} \tag{4}$$

In general, due to the presence of the interference from the PU, there does not exist an effective method to calculate C_{s}, C_{f}, and $P_{\text{out}}(r)$. Even for the static channel, the calculation of C_{s} in [16] was relied on some rough approximations and the accuracy might be an issue. It is because the calculation in [16] relied on specific levels of signal-to-noise ratio (SNR). In the subsequent sections, we shall introduce new methods to evaluate C_{s}, C_{f}, and $P_{\text{out}}(r)$ in an effective manner to achieve any level of accuracy.

3 Achievable rates of CR static channel

In this section, the focus is on the calculation of C_{s} for the static channel. Instead of relying on approximate calculations [16], we will show that C_{s} can be expressed in closed-form using a simple series representation and we can achieve any level of accuracy.

Let us start with the differential entropy of the total noise $h(\boldsymbol{n}_{\text{T}})$. Using the same analysis as in [16], we have

$$\begin{aligned} h(\boldsymbol{n}_{\text{T}}) &= -\mathbb{E}\left[\log\left(f_{n_{\text{T}}}(n_{\text{R}}, n_{\text{I}})\right)\right] \\ &= \log\left(\frac{2\pi(\sigma_n^2+\sigma_I^2)}{p_1}\right) + \log(e)\left(\frac{\sigma_n^2+p_1\sigma_I^2}{\sigma_n^2+\sigma_I^2}\right) - \Upsilon(n_{\text{R}}, n_{\text{I}}). \end{aligned} \tag{5}$$

where n_{R} and n_{I}, respectively, denote real and imaginary components of $\boldsymbol{n}_{\text{T}}$, and

$$\Upsilon(n_{\text{R}}, n_{\text{I}}) = \int_0^\infty \int_0^\infty \log\left[1+\delta\exp\left(-\frac{n_{\text{R}}^2+n_{\text{I}}^2}{2\sigma_n^2}\right)\right] f_{\boldsymbol{n}_{\text{T}}}(n_{\text{R}}, n_{\text{I}})\, \text{d}n_{\text{R}}\, \text{d}n_{\text{I}} \tag{6}$$

In (6), we denote $\delta = (1-p_1)(\sigma_n^2+\sigma_I^2)/p_1\sigma_n^2$ and $1/\sigma^2 = (1/\sigma_n^2) - (1/(\sigma_n^2+\sigma_I^2))$. Furthermore, $f_{\boldsymbol{n}_{\text{T}}}(\cdot,\cdot)$ is the joint probability density function (PDF) of n_{R} and n_{I} and is given as

$$\begin{aligned} f_{n_{\text{T}}}(n_{\text{R}}, n_{\text{I}}) &= \frac{(1-p_1)}{2\pi\sigma_n^2}\text{e}^{-(n_{\text{R}}^2+n_{\text{I}}^2)/2\sigma_n^2} \\ &\quad + \frac{p_1}{2\pi(\sigma_n^2+\sigma_I^2)}\text{e}^{-(n_{\text{R}}^2+n_{\text{I}}^2)/2(\sigma_n^2+\sigma_I^2)}. \end{aligned} \tag{7}$$

Using the polar coordinator $n_{\text{R}} = r\cos(\phi)$ and $n_{\text{I}} = r\sin(\phi)$, (6) can be further expressed as

$$\Upsilon(n_{\text{R}}, n_{\text{I}}) = \frac{\log(e)}{2}\left[\frac{(1-p_1)}{\sigma_n^2}I_1 + \frac{p_1}{\sigma_n^2+\sigma_I^2}I_2\right] \tag{8}$$

where

$$I_i = \int_0^\infty \ln\left(1+\delta\text{e}^{-\varphi x}\right)\text{e}^{-\beta_i x}\, \text{d}x,$$

with $i = \{1, 2\}$, $x = r^2$, $\varphi = 1/2\sigma^2$, $\beta_1 = 1/2\sigma_n^2$, and $\beta_2 = 1/2(\sigma_n^2+\sigma_I^2)$. Now, let $y = \varphi x - \ln\delta$ and $\mu = \beta_1/\varphi = \sigma^2/\sigma_n^2$. The parameter I_1 can then be expressed as

$$I_1 = \frac{\text{e}^{-\mu\ln\delta}}{\varphi}\int_{-\ln\delta}^\infty \ln(1+\text{e}^{-y})\text{e}^{-\mu y}\, \text{d}y. \tag{9}$$

Using integration by parts with $u = \ln(1+\text{e}^{-y})$ and $\text{d}v = \text{e}^{-\mu y}\,\text{d}y$, we obtain $\text{d}u = -(\text{e}^{-y}/(1+\text{e}^{-y}))\text{d}y$ and $v = -\text{e}^{-\mu y}/\mu$. Applying this transformation to (9), we have

$$\begin{aligned} I_1 &= \frac{\text{e}^{-\mu\ln\delta}}{\varphi}\int_{-\ln\delta}^\infty u\, \text{d}v \\ &= \frac{\ln(1+\delta)}{\beta_1} - \frac{\delta^{-\mu}}{\beta_1}\int_{-\ln\delta}^\infty \frac{\text{e}^{-(\mu+1)y}}{(1+\text{e}^{-y})}\, \text{d}y. \end{aligned} \tag{10}$$

Now, let $z = \text{e}^{-y}/(1+\text{e}^{-y})$. I_1 in (10) can be then calculated as

$$\begin{aligned} I_1 &= \frac{\ln(1+\delta)}{\beta_1} - \frac{\delta^{-\mu}}{\beta_1}\int_0^{\delta/(1+\delta)} z^\mu(1-z)^{-(1+\mu)}\, \text{d}z \\ &\overset{(a)}{=} \frac{\ln(1+\delta)}{\beta_1} - \frac{\delta^{-\mu}}{\beta_1}x^a\int_0^1 u^{a-1}(1-ux)^{-a}\, \text{d}u \\ &\overset{(b)}{=} \frac{\ln(1+\delta)}{\beta_1} - \frac{\delta^{-\mu}}{\beta_1}x^a\int_0^1 \left(\frac{1-t}{1-xt}\right)^{a-1}\left[1-\frac{x(1-t)}{1-xt}\right]^{-a}\frac{(1-x)}{(1-xt)^2}\, \text{d}t \\ &= \frac{\ln(1+\delta)}{\beta_1} - \frac{\delta^{-\mu}}{\beta_1}x^a\int_0^1 \left(\frac{1-t}{1-xt}\right)^{a-1}\left(\frac{1-x}{1-xt}\right)^{-a}\frac{(1-x)}{(1-xt)^2}\, \text{d}t \\ &= \frac{\ln(1+\delta)}{\beta_1} - \frac{\delta^{-\mu}}{\beta_1}x^a(1-x)^{-(a-1)}\int_0^1 \frac{(1-t)^{a-1}}{1-xt}\, \text{d}t \\ &= \frac{\ln(1+\delta)}{\beta_1} - \frac{x}{\beta_1}\int_0^1 \frac{(1-t)^{a-1}}{1-xt}\, \text{d}t \end{aligned} \tag{11}$$

where $x = \delta/(1+\delta)$, $a = \mu+1$, and $u = z/x$ in (a). Furthermore, in (b), we set $t = (1-u)/(1-xu)$, which yields $u = (1-t)/(1-xt)$ and $\text{d}u = -((1-x)/(1-zt)^2)\text{d}t$. Using the geometric series representation of the term $1/(1-xt)$ in (11), we then obtain

$$\begin{aligned} I_1 &= \frac{\ln(1+\delta)}{\beta_1} - \frac{x}{\beta_1}\int_0^1 (1-t)^{a-1}\sum_{n=0}^\infty (xt)^n\, \text{d}t \\ &\overset{(c)}{=} \frac{\ln(1+\delta)}{\beta_1} - \frac{1}{\beta_1}\sum_{n=0}^\infty x^{n+1}\int_0^1 v^{a-1}(1-v)^n\, \text{d}v \\ &\overset{(d)}{=} \frac{\ln(1+\delta)}{\beta_1} - \frac{1}{\beta_1}\sum_{n=0}^\infty x^{n+1}\int_0^1 \sum_{k=0}^n (-1)^k\binom{n}{k}v^{a+k-1}\, \text{d}v \\ &= \frac{\ln(1+\delta)}{\beta_1} - \frac{1}{\beta_1}\sum_{n=0}^\infty\sum_{k=0}^n \binom{n}{k}\frac{(-1)^k x^{n+1}}{k+\mu+1}. \end{aligned} \tag{12}$$

Note that in (c), we change the parameter $v = 1-t$ and in (d), we apply the binomial series representation $(1+x)^\alpha = \sum_{k=0}^\infty \binom{\alpha}{k}x^k$. As we show in the Appendix, the truncation of the first N terms from $n=0$ to $n=(N-1)$ will introduce an error that is upper-bounded by

$$\text{error} < \frac{1}{\beta_1}\sum_{n=N}^\infty \frac{x^{n+1}}{\mu+1} = \frac{1}{\beta_1(\mu+1)}\left(\frac{x^{N+1}}{1-x}\right). \tag{13}$$

Since $x \in (0,\ 1)$, it can be seen that the error decreases as N increases and it converges to zero when $N \to \infty$. Therefore, the calculation of I_1 can be done with any accuracy level. In particular, for a given error

IET Commun., 2015, Vol. 9, Iss. 17, pp. 2160–2167

level ϵ, one can use the first $N_1^{n_T} = \left\lceil \frac{\ln(\epsilon\beta_1(\mu+1)(1-x))}{\ln x} - 1 \right\rceil$ terms to achieve an error that is smaller than ϵ.

Using a similar procedure, we can obtain I_2 in (5) by replacing β_1 and μ in I_1 by β_2 and $\lambda = \beta_2/\varphi = \sigma^2/(\sigma_n^2 + \sigma_I^2)$, respectively. For I_2, to achieve an error that is smaller than ϵ, we can use the first $N_2^{n_T} = \left\lceil \frac{\ln(\epsilon\beta_2(\lambda+1)(1-x))}{\ln x} - 1 \right\rceil$ terms in the series representation.

Combining with I_1 calculated earlier, we obtain the closed-form expression of the entropy of $\boldsymbol{n}_T$, which is given in (14)

$$\begin{aligned} h(\boldsymbol{n}_T) &= \log\left(\frac{2\pi\sigma_n^2(\sigma_n^2+\sigma_I^2)}{\sigma_n^2+(1-p_1)\sigma_I^2}\right) + \log(e)\left(\frac{\sigma_n^2+p_1\sigma_I^2}{\sigma_n^2+\sigma_I^2}\right) \\ &\quad + \log(e)\left(\frac{(1-p_1)\sigma_n^2\sigma_I^2}{\sigma_n^2\sigma_I^2+\sigma_n^2(\sigma_n^2+\sigma_I^2)}\right)\sum_{n=0}^{\infty}\sum_{k=0}^{n}\binom{n}{k} \\ &\quad \frac{(-1)^k\left((1-p_1)(\sigma_n^2+\sigma_I^2)/((1-p_1)\sigma_I^2+\sigma_n^2)\right)^{n+1}}{k+1+\left((\sigma_n^2+\sigma_I^2)/\sigma_I^2\right)} \\ &\quad + \log(e)\left(\frac{p_1\sigma_I^2}{\sigma_n^2+\sigma_I^2}\right)\sum_{n=0}^{\infty}\sum_{k=0}^{n}\binom{n}{k} \\ &\quad \frac{(-1)^k\left((1-p_1)(\sigma_n^2+\sigma_I^2)/((1-p_1)\sigma_1^2+\sigma_n^2)\right)^{n+1}}{k+1+(\sigma_n^2/\sigma_I^2)} \end{aligned} \tag{14}$$

It is not hard to verify that by using the first $N_{n_T} = \max(N_1^{n_T}, N_2^{n_T})$ in the two series in (14), the maximum error in the approximation of $h(\boldsymbol{n}_T)$ is

$$\epsilon_{n_T} = \epsilon\frac{\log(e)}{2}\left[\frac{(1-p_1)(\sigma_n^2+\sigma_I^2)+p_1\sigma_n^2}{\sigma_n^2(\sigma_n^2+\sigma_I^2)}\right]. \tag{15}$$

Now, turning our attention to the differential entropy of the output, it is easy to show that the moment generating function of the output is

$$\phi_y(\omega_1, \omega_2) = e^{-(1/2)\beta\left(\omega_1^2+\omega_2^2\right)}\left(1-p_1+p_1e^{-(1/2)\sigma_I^2\left(\omega_1^2+\omega_2^2\right)}\right), \tag{16}$$

where $\beta = (P_x/p_e) + \sigma_n^2$. Then, taking the inverse Fourier transform of (16) yields the PDF of $\boldsymbol{y}_{GI}$ as

$$\begin{aligned} f_y(y_R, y_I) &= \frac{(1-p_1)}{2\pi\beta}e^{-(y_R^2+y_I^2)/2\sigma_n^2} \\ &\quad + \frac{p_1}{2\pi(\beta+\sigma_I^2)}e^{-(y_R^2+y_I^2)/2\left(\beta+\sigma_I^2\right)}, \end{aligned} \tag{17}$$

where y_R and y_I are the real and imaginary components of the joint PDF of $\boldsymbol{y}_{GI}$. Therefore, the differential entropy of $\boldsymbol{y}_{GI}$ can be represented as

$$\begin{aligned} h(\boldsymbol{y}) &= -\mathbb{E}[\log(f_y(y_R, y_I))] \\ &= \log\left(\frac{2\pi(\beta+\sigma_I^2)}{p_1}\right) + \log(e)\left(\frac{\beta+p_1\sigma_I^2}{\beta+\sigma_I^2}\right) - \Upsilon(y_R, y_I). \end{aligned} \tag{18}$$

where

$$\Upsilon(y_R, y_I) = \int_0^{\infty}\int_0^{\infty}\log\left[1+\delta\exp\left(-\frac{y_R^2+y_I^2}{2\beta}\right)\right]f_y(y_R, y_I)\,dy_R\,dy_I \tag{19}$$

Observe that the differential entropy $h(\boldsymbol{y})$ in (18) has the same form with the differential entropy of the total noise in (5). By replacing σ_n^2 in (5) by β, we obtain the differential entropy $h(\boldsymbol{y})$ in a simple series representation as follows

$$\begin{aligned} h(\boldsymbol{y}) &= -\mathbb{E}[\log(f_y(y_R, y_I))] \\ &= \log\left(\frac{2\pi(\beta+\sigma_I^2)}{p_1}\right) + \log(e)\left(\frac{\beta+p_1\sigma_I^2}{\beta+\sigma_I^2}\right) \\ &\quad + \log(e)\frac{(1-p_1)\beta\sigma_I^2}{(\beta\sigma_I^2+\beta(\beta+\sigma_I^2))} \\ &\quad \times\sum_{n=0}^{\infty}\sum_{k=0}^{\infty}\binom{n}{k}\frac{(-1)^k\left((1-p_1)(\beta+\sigma_I^2)/((1-p_1)\sigma_I^2+\beta)\right)^{n+1}}{k+1+\left((\beta+\sigma_I^2)/\sigma_I^2\right)} \\ &\quad + \log(e)\frac{(p_1)\sigma_I^2}{(\beta+\sigma_I^2)}\times\sum_{n=0}^{\infty}\sum_{k=0}^{\infty}\binom{n}{k} \\ &\quad \frac{(-1)^k\left((1-p_1)(\beta+\sigma_I^2)/((1-p_1)\sigma_I^2+\beta)\right)^{n+1}}{k+1+(\beta/\sigma_I^2)}. \end{aligned} \tag{20}$$

As similar to the analysis for $h(\boldsymbol{n}_T)$, it can be verified that by using the first $N_y = \max(N_1^y, N_2^y)$ in the two series in (20), the maximum error in the approximation of $h(\boldsymbol{y})$ is

$$\epsilon_y = \epsilon\frac{\log(e)}{2}\left[\frac{(1-p_1)(\beta+\sigma_I^2)+p_1\beta}{\beta(\beta+\sigma_I^2)}\right]. \tag{21}$$

Here, N_1^y and N_2^y can be calculated as similar to $N_1^{n_T}$ and $N_2^{n_T}$ by replacing σ_n^2 by β in calculating β_1, β_2, μ, λ, and x.

Finally, substituting $h(\boldsymbol{y})$ and $h(\boldsymbol{n}_T)$ into (2) yields the achievable rate C_s in closed-form. The truncation of the first $N = \max(N_y, N_{n_T})$ terms in the four series representations result in a maximum error of $\max(\epsilon_y, \epsilon_{n_T})$.

4 Achievable rates and outage probability of CR Rayleigh fading channel

In this section, we consider the CR SU link in a wireless fading environment. We first focus on the calculation of the ergodic achievable rate in fast fading before extending to the computation of the outage probability in slow fading.

4.1 Calculation of C_f

Observe from (3) that the key point in obtaining C_f is to calculate the differential entropy $h(\boldsymbol{y})$ averaged over g. It is because the differential entropy $h(\boldsymbol{n}_T)$ can be effectively calculated as in the previous section. For a given g, we can treat the channel as a static channel. As such, the instantaneous differential entropy of the output $h(\boldsymbol{y}|g)$ of the considered CR link can be expressed in closed-form by replacing σ_n^2 in (14) by $\kappa(g) \triangleq \left(|g|^2(P_x/p_e) + \sigma_n^2\right)$. Since $h(\boldsymbol{y}|g)$ is a function of $\alpha = |g|^2$, with a slight abuse of notation, hereafter, let us denote $h(\boldsymbol{y}|g)$ as $h(\boldsymbol{y}|\alpha)$ and $\kappa(g)$ as $\kappa(\alpha)$, respectively. Note that α follows the exponential distribution, that is, $p(\alpha) = e^{-\alpha}$. We then have

$$h(\boldsymbol{y}) = \int_0^{\infty} h(\boldsymbol{y}|\alpha)e^{-\alpha}\,d\alpha. \tag{22}$$

Given that $h(\boldsymbol{y}|\alpha)$ can be easily calculated for a given α using the simple series representation derived earlier, we can adopt the PLCF method in [22] to evaluate the integral in (22). The main idea of PLCF is to approximately represent a curve using linear segments in which we can control the gap between the curve and the segments with any given accuracy level. However, the PLCF method can only be applied to a curve consisting of finite values.

Since $h(\boldsymbol{y}|\alpha)$ is not finite when α goes to ∞, the PLCF method cannot be used directly. Our idea is to approximate $h(\boldsymbol{y}|\alpha)$ by a simple function of α when α is beyond a certain threshold α_{th} that depends on the accuracy level, and to approximate $h(\boldsymbol{y}|\alpha)$ using PLCF when $\alpha < \alpha_{\text{th}}$. To this end, we consider the use of an upper-bound on the achievable rate derived in [16] under the assumption of a Gaussian output. In particular, if the output is Gaussian distributed, for a given α, the differential entropy of the output can be expressed as

$$h_{\text{GO}}(\alpha) = \log\big(2\pi e\big(\kappa(\alpha) + p_1\sigma_I^2\big)\big). \tag{23}$$

While $h_{\text{GO}}(\alpha)$ is an upper-bound on $h(\alpha) \triangleq h(\boldsymbol{y}|\alpha)$, it is observed via numerical results in [16] that $h(\alpha)$ approaches $h_{\text{GO}}(\alpha)$ when α goes to ∞. To further evaluate the difference between $h_{\text{GO}}(\alpha)$ and $h(\alpha)$, we first express $h(\alpha)$ as follows

$$h(\alpha) = \log\left[\frac{2\pi\kappa(\alpha)\big(\kappa(\alpha)+\sigma_I^2\big)}{\kappa(\alpha)+(1-p_1)\sigma_I^2}\right] + \log(e)\frac{\kappa(\alpha)+p_1\sigma_I^2}{\kappa(\alpha)+\sigma_I^2} - \Upsilon'(y_{\text{R}},\, y_{\text{I}}) \tag{24}$$

where $\Upsilon'(y_{\text{R}}, y_{\text{I}})$ is obtained by replacing σ_n^2 in (6) by $\kappa(\alpha)$. Since $0 < \exp\big(-(y_{\text{R}}^2+y_{\text{I}}^2)/2\kappa(\alpha)\big) \le 1$ for $-\infty < y_{\text{R}},\ y_{\text{I}} < \infty$, $\Upsilon'(y_{\text{R}}, y_{\text{I}})$ can be upper-bounded by

$$\Upsilon'(y_{\text{R}},\, y_{\text{I}}) \le \log\left(1 + \frac{(1-p_1)\big(\kappa(\alpha)+\sigma_I^2\big)}{p_1\kappa(\alpha)}\right). \tag{25}$$

Then, from (24), we obtain the lower bound on $h(\alpha)$

$$h(\alpha) > \log\left[\frac{2\pi\kappa(\alpha)\big(\kappa(\alpha)+\sigma_I^2\big)}{\kappa(\alpha)+(1-p_1)\sigma_I^2}\right] + \log(e)\frac{\kappa(\alpha)+p_1\sigma_I^2}{\kappa(\alpha)+\sigma_I^2}. \tag{26}$$

Using this result, the difference between $h_{\text{GO}}(\alpha)$ and $h(\alpha)$, $\Delta h = h_{\text{GO}}(\alpha) - h(\alpha)$, can be upper-bounded as follows

$$\begin{aligned}\Delta h &< \log\left(1 + \frac{p_1(1-p_1)\sigma_I^4}{\kappa(\alpha)\big(\kappa(\alpha)+\sigma_I^2\big)}\right) + \log(e)\frac{(1-p_1)\sigma_I^2}{\kappa(\alpha)+\sigma_I^2} \\ &< \log(e)\left[\frac{(1-p_1)\big(\kappa(\alpha)+p_1\sigma_I^2\big)}{\kappa(\alpha)+\sigma_I^2}\right]\cdot\frac{\sigma_I^2}{\kappa(\alpha)} \qquad (27a) \\ &\le \frac{\log(e)(1-p_1)\sigma_I^2}{\kappa(\alpha)}, \qquad (27b)\end{aligned}$$

where (27a) is achieved by using the inequality $\ln(1+x) < x$ with $x > 0$ and (27b) follows the fact that $(\kappa(\alpha)+p_1\sigma_I^2)/(\kappa(\alpha)+\sigma_I^2) \le 1$ for $\alpha \ge 0$ and $0 \le p_1 \le 1$.

Observe that the upper-bound on Δh in (27b) is a decreasing function of α. For a given error tolerance ϵ, it can be easily verified that if we choose α_{th} such that $\log(e)(1-p_1)\sigma_I^2/\kappa(\alpha_{\text{th}}) = \epsilon$, or equivalently, $\alpha_{\text{th}} = p_e\big((\log(e)(1-p_1)\sigma_I^2/\epsilon P_x) - (\sigma_n^2/P_x)\big)$, the difference Δh is smaller than ϵ for $\alpha \ge \alpha_{\text{th}}$.

Since α_{th} is a fixed value, $h(\alpha)$ is finite for $\alpha < \alpha_{\text{th}}$. In this case, we can apply the PLCF method to approximate $h(\alpha)$ using linear segments in which the approximation error is always upper-bounded by the chosen error tolerance ϵ. Specifically, the approximation of $h(\alpha)$ can be expressed in the form of linear segments as follows

$$h(\alpha) \simeq a_m\alpha + b_m, \quad \text{for} \quad \alpha_{m-1} < \alpha \le \alpha_m, \tag{28}$$

where $m = 1, \ldots, M$, $\alpha_0 = 0$, and $\alpha_M = \alpha_{\text{th}}$. Note that a_m and b_m, respectively, are the slope and intercept of the mth segment $(\alpha_{m-1}, \alpha_m]$ of the PLCF.

Given the above approximations with controllable error levels, we can now proceed to evaluate the average achievable rate C_{f}. By using PLCF in the range $(0,\ \alpha_{\text{th}}]$ and using $h(\alpha) = h_{\text{GO}}(\alpha)$ in the range $[\alpha_{\text{th}}, \infty)$, we obtain the following approximation on the entropy $h(\boldsymbol{y})$

$$\begin{aligned}h(\boldsymbol{y}) &\simeq \sum_{m=1}^{M}\int_{\alpha_{m-1}}^{\alpha_m}(a_m\alpha + b_m)\mathrm{e}^{-\alpha}\,\mathrm{d}\alpha \\ &\quad + \int_{\alpha_M}^{\infty}\log\big(2\pi e\big(\kappa(\alpha)+p_1\sigma_I^2\big)\big)\mathrm{e}^{-\alpha}\,\mathrm{d}\alpha \triangleq A + B. \end{aligned}\tag{29}$$

where A is the summation of the first M integrals and B is the last integral in (29). To evaluate A in (29), we represent the integrals using series representations as follows

$$\begin{aligned}A &= \sum_{m=1}^{M}\int_{\alpha_{m-1}}^{\alpha_m}(a_m\alpha + b_m)\mathrm{e}^{-\alpha}\,\mathrm{d}\alpha \\ &= \sum_{m=1}^{M}a_m\mathrm{e}^{-\alpha}(1+\alpha)\Big|_{\alpha=\alpha_m}^{\alpha=\alpha_{m-1}} + \sum_{m=1}^{M}b_m\mathrm{e}^{-\alpha}\Big|_{\alpha=\alpha_m}^{\alpha=\alpha_{m-1}}\end{aligned}\tag{30}$$

where we have used the following integral

$$\int_a^b x^n\mathrm{e}^{-x}\,\mathrm{d}x = -\mathrm{e}^{-x}n!\sum_{i=0}^{n}\frac{x^i}{i!}\Big|_{x=a}^{x=b} \tag{31}$$

for $n = 0$ and $n = 1$.

Next, we can write the last integral B in (29) as follows

$$\begin{aligned}B &= \int_{\alpha_M}^{\infty}\log\big(2\pi e\big(\kappa(\alpha)+p_1\sigma_I^2\big)\big)\mathrm{e}^{-\alpha}\,\mathrm{d}\alpha \\ &= \int_{\alpha_M}^{\infty}\log\big(2\pi e\big(\sigma_n^2+p_1\sigma_I^2\big)\big)\mathrm{e}^{-\alpha}\,\mathrm{d}\alpha + \int_{\lambda}^{\infty}\log(\alpha'+1)\nu\mathrm{e}^{-\nu\alpha'}\,\mathrm{d}\alpha' \\ &= \log\big(2\pi e\big(\sigma_n^2+p_1\sigma_I^2\big)\big)\mathrm{e}^{-\alpha_M} \\ &\quad + \log(\lambda+1)\mathrm{e}^{-\nu\lambda} + \log(e)\mathrm{e}^{\nu}E_1(\nu(\lambda+1)),\end{aligned}\tag{32}$$

where $\lambda = \alpha_M P_x/p_e\big(\sigma_n^2+p_1\sigma_I^2\big)$, $\nu = p_e\big((\sigma_n^2+p_1\sigma_I^2)/P_x\big)$, $\alpha' = \alpha\big(P_x/p_e\big(\sigma_n^2+p_1\sigma_I^2\big)\big)$, and $E_1(\cdot)$ is the exponential integral $E_1(z) = \int_1^{\infty}\mathrm{e}^{-tz}/t\,\mathrm{d}t$. In (32), the last equality is obtained using the integral [23, eq. (4.337.1)].

By substituting A and B from (30) and (32) into (22), we obtain the closed-form approximation of the differential entropy $h(\boldsymbol{y})$ as

$$\begin{aligned}h(\boldsymbol{y}) &\simeq \sum_{m=1}^{M}(a_m+b_m)\big(\mathrm{e}^{-\alpha_{m-1}} - \mathrm{e}^{-\alpha_m}\big) + \sum_{m=1}^{M}a_m\big(\alpha_{m-1}\mathrm{e}^{-\alpha_{m-1}} - \alpha_m\mathrm{e}^{-\alpha_m}\big) \\ &\quad + \log\big(2\pi e\big(\kappa(\alpha_M)+p_1\sigma_I^2\big)\big)\mathrm{e}^{-\alpha_M} \\ &\quad + \log(e)\mathrm{e}^{p_e\left((\sigma_n^2+p_1\sigma_I^2)/P_x\right)}E_1\left(\alpha_M + p_e\frac{\sigma_n^2+p_1\sigma_I^2}{P_x}\right).\end{aligned}\tag{33}$$

It can be verified that the calculation in (33) results in an average error $\bar{\epsilon}$ that will not exceed ϵ. Finally, by substituting the differential entropies $h(\boldsymbol{n}_\Gamma)$ and $h(\boldsymbol{y})$ from (14) and (33) into (3), we obtain the achievable rate C_{f}.

4.2 Calculation of outage probability

Now, for the outage probability in (4), it can be expressed as follows

$$P_{\text{out}}(r) = \Pr\{h(\boldsymbol{y}|g) - h(\boldsymbol{n}_\Gamma) \le r\} = \Pr\{\gamma \le \gamma_{\min}\} \triangleq F_\gamma(\gamma_{\min}) \tag{34}$$

where $\gamma_{\min}$ is the minimum required value of the received SNR in

order to achieve the target rate r, $\gamma \triangleq \alpha\Gamma$ is the received SNR, and $F_\gamma(\cdot)$ is the cumulative distribution function of γ. Since γ follows the exponential distribution, we then have

$$P_{\text{out}}(r) = \Pr\{h(\boldsymbol{y}|g) - h(\boldsymbol{n}_\Gamma) \le r\} = 1 - \exp\left[-\frac{\gamma_{\min}}{\Gamma}\right] \tag{35}$$

For a desired rate r, the outage probability $P_{\text{out}}(r)$ can be calculated by finding the minimum SNR $\gamma_{\min}$ to achieve the rate r. To this end, we can apply the PLCF-based method to approximate $\gamma_{\min}$ for a pre-determined error level. In particular, for a given r, it is easy to calculate $(r + p_e h(\boldsymbol{n}_\Gamma))/p_e$. That gives us a specific value of $h(\boldsymbol{y}|g)$. Now, using the PLCF technique, we can find the slope and intercepts a_m and b_m of the linear segment that $h(\boldsymbol{y}|g)$ belongs, which is given as $a_m\gamma + b_m$. As a result, $\gamma_{\min}$ can be approximated as

$$\gamma_{\min} \cong \frac{1}{a_m}\left[\frac{r}{p_e} - b_m + h(\boldsymbol{n}_\Gamma)\right] \tag{36}$$

where the value of m is such that $r_{m-1} < r \le r_m$. For completeness, we have provided the slope and intercept values a_m and b_m, respectively, in Table 1 with the accuracy $\epsilon = 0.01$. The outage probability can then be effectively calculated as

$$P_{\text{out}}(r) = 1 - \exp\left[-\left(\frac{r}{p_e} - b_m + h(\boldsymbol{n}_\Gamma)\right)\frac{1}{a_m\Gamma}\right]. \tag{37}$$

Given the above expression for the outage probability, one can also obtain an alternative performance measure referred to as $\varepsilon-$outage capacity [24]. This value can be understood as the maximum data rate that can be achieved such that the outage probability is less than ε. By solving $P_{\text{out}}(r) = \varepsilon$, it is straightforward see that this $\varepsilon-$outage capacity can be expressed in closed-form as

$$C_{\text{out}}(\varepsilon) = p_e\left[-a_m\Gamma\log(1-\varepsilon) + b_m - h(\boldsymbol{n}_\Gamma)\right]. \tag{38}$$

5 Numerical results

This section provides numerical results to verify the theoretical derivations and calculations in the previous sections. In all the results for the achievable rate, it is drawn versus the average SNR, $\Gamma = P_x/\sigma_n^2$. The value of interference-to-noise ratio $\xi = \sigma_I^2/\sigma_n^2$ is set at 20 dB, unless otherwise stated. For all of the figures, the values of $P_{\text{m}} = P_{\text{f}} = 0.1$ are selected. These values are specified as the maximum tolerable limit of sensing imperfectness in the CR standard IEEE 802.22 [20]. It is also worth mentioning that in practice, P_{m} and P_{f} depend on a given sensing technique and the proposed method can be applied to any P_{m} and P_{f}. When using the proposed series presentations to calculate the total noise entropy, the output entropy, and the rate, we follow the selection criteria discussed in Section 3. A to select the number of terms N in the series representation to achieve high accuracy. Such selection is SNR dependent and N can run from a few hundreds to a few thousands in the SNR's range of interest. Since (15) and (21) are the upper bounds on the approximation errors, we observe that the use of the first $N = 1000$ terms in any series representation is sufficient. This value is therefore adopted in all calculations.

Table 1 Coefficients for the PLCF as a function of SNR with error tolerance $\epsilon = 0.01$

M	r_{m+1}	Slope (a_m)	Intercept (b_m)
1	0.3059428065	1.2382829816	3.2340169676
2	0.6184785530	0.9611303983	3.3171710663
3	0.9185473304	0.7296250082	3.4792410626
4	1.2396824871	0.5648865760	3.6769469716
5	1.5836106365	0.4201288158	3.9520142502
6	1.9391502641	0.3107991046	4.2691021532
7	2.3097001108	0.2265676063	4.6313338551
8	2.6849514800	0.1635014990	5.0286901069
9	3.0620405973	0.1179992878	5.4428016811
10	3.4447083244	0.08494261126	5.8725814981
11	3.8294539164	0.06092874895	6.3168824254
12	4.2168626682	0.04376901783	6.7665123886
13	4.6057323031	0.03140112866	7.2241700994
14	4.9959626147	0.02255873865	7.6849047385
15	5.3876827956	0.01619452593	8.1508117471
16	5.7802877795	0.01162143328	8.6205153803
17	6.1733602041	0.00833635638	9.0932852697
18	6.5670017584	0.00597835135	9.5682350248
19	6.9609352208	0.00428518388	10.045248052
20	7.3548793821	0.00307145685	10.523261602

5.1 Achievable rates of CR static channel

We first demonstrate the accuracy of the calculation of the achievable rate over the static channel. Fig. 2 plots the achievable rate C_{s} calculated from (2) using the series representation of $h(\boldsymbol{n}_\Gamma)$ in (14) and the series representation of $h(\boldsymbol{y})$ in (20) for three different probabilities of the presence of PU, $p = 0.1$, $p = 0.2$, and $p = 0.5$. For comparison, the achievable rates obtained by Monte Carlo simulations are also provided. For the Monte Carlo simulations, at a given P_x, σ_I^2, and σ_n^2, 10^7 samples of the total noise plus interference $\boldsymbol{n}_\Gamma = b_m I + \boldsymbol{n}$ are generated, together with the same number of samples of the input $\boldsymbol{x}$. Note that $\boldsymbol{I}$, $\boldsymbol{n}$, and $\boldsymbol{x}$ are all complex Gaussian, while b_m is generated according to a Bernoulli distribution with $\mathcal{P}(b_m = 1) = pP_{\text{m}} \triangleq p_1$. Then 10^7 samples of the output $\boldsymbol{y}$ are created using $\boldsymbol{y} = \boldsymbol{x} + \boldsymbol{n}$. From the complex samples of the total noise plus interference $\boldsymbol{n}_\Gamma$, the differential entropy $h(\boldsymbol{n}_\Gamma)$ is calculated by averaging over 10^7 values of $-\log(f_{n_\Gamma}(n_{\text{R}}, n_{\text{I}}))$. The differential entropy $h(\boldsymbol{y})$ for given $b_e = 1$ can be calculated in a similar manner using $-\log(f_y(y_{\text{R}}, y_{\text{I}}))$. The achievable rate can then be obtained as $h(\boldsymbol{y}) - h(\boldsymbol{n}_\Gamma)$. It can be observed from Fig. 2 that the proposed calculation matches perfectly with Monte Carlo simulations. As a result, it can be used effectively to predict the achievable rate without the need of lengthy Monte Carlo simulations.

5.2 Ergodic achievable rates in Rayleigh fading

Extending the results to the Rayleigh fading channel, we first evaluate the ergodic achievable rates in fast fading. In Figs. 3 and 4, we compare the approximation of the proposed PLCF-based method with Monte Carlo simulation results for two accuracy levels, $\epsilon = 0.1$ and 0.01, respectively. In all cases, the achievable rate curves are obtained for three different values of p, $p = 0.1$, $p = 0.2$, and $p = 0.5$. Note that with Monte Carlo simulations, we

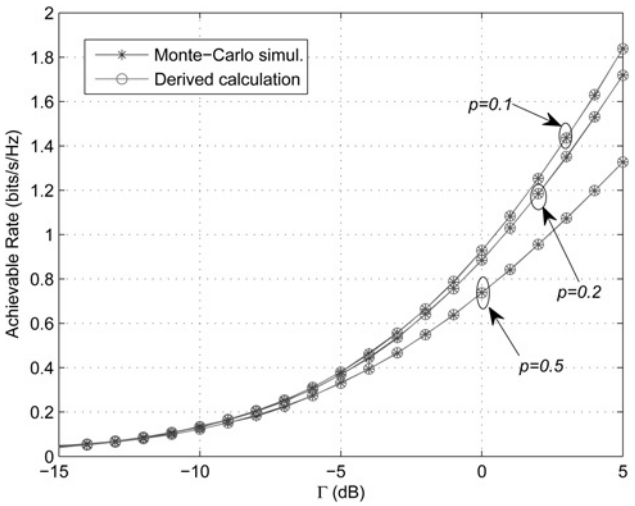

Fig. 2 *Achievable rate C_s of the CR link obtained from the derived calculation and Monte Carlo simulations over the static channel for different values of p*

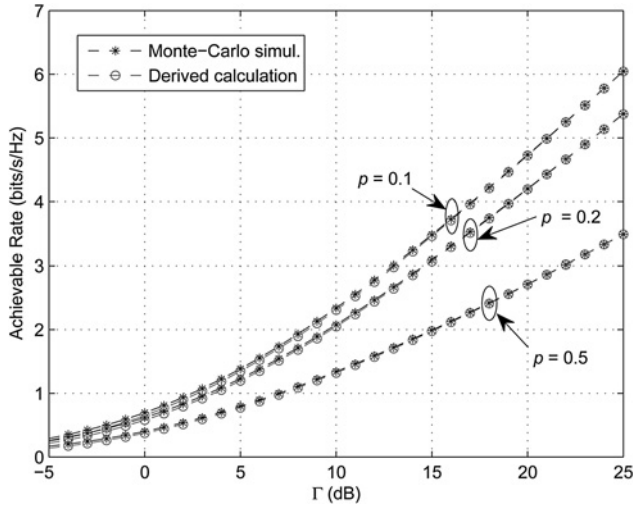

Fig. 3 *Achievable rate C_f obtained from Monte Carlo simulations and the derived calculation over Rayleigh fading with different values of p and $\epsilon = 0.1$*

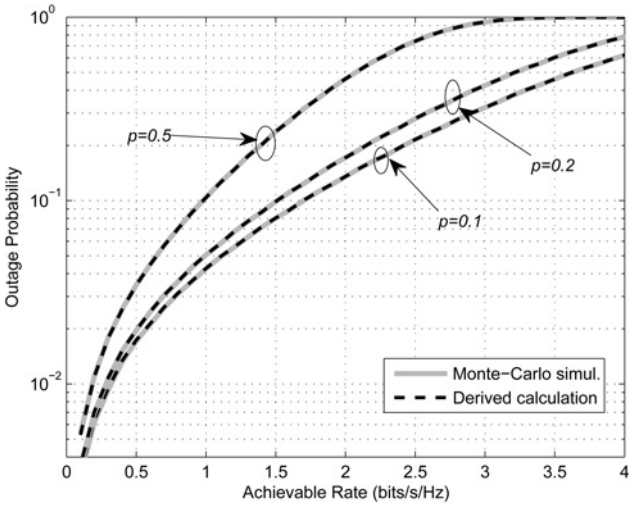

Fig. 5 *Outage probability for Rayleigh fading channel for different values of p. The average SNR Γ is set at 15 dB*

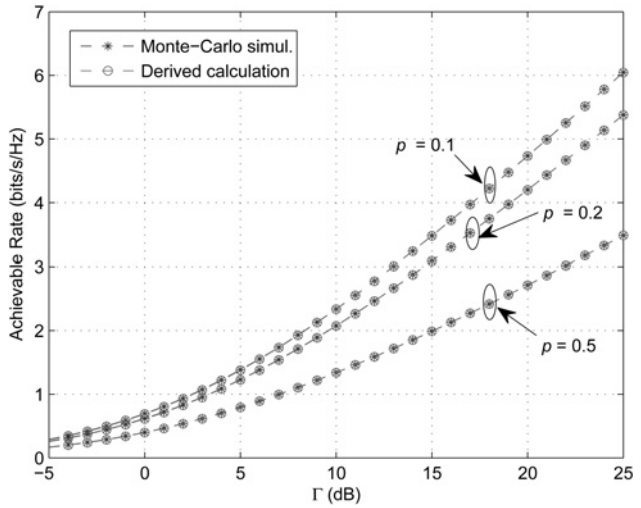

Fig. 4 *Achievable rate C_f obtained from Monte Carlo simulations and the derived calculation over Rayleigh fading with different values of p and $\epsilon = 0.01$*

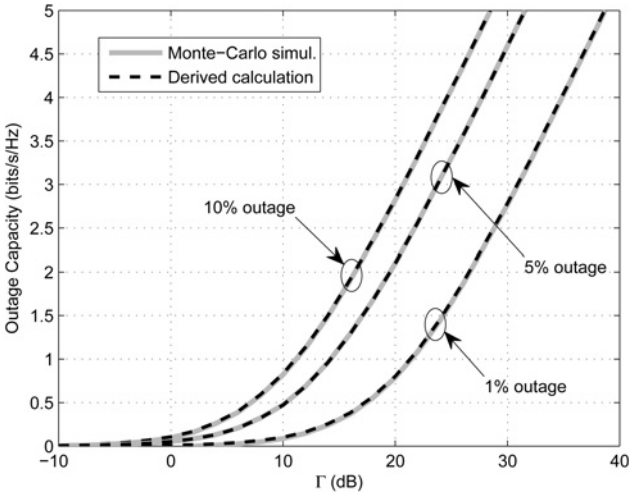

Fig. 6 *Outage capacity with 1, 5, and 10% outage obtained from Monte Carlo simulations and the derived calculation over slow Rayleigh fading with $p = 0.1$ and $\epsilon = 0.01$*

generate the same number of samples of the channel gain g. Then 10^7 samples of the output $\boldsymbol{y}$ are created using $\boldsymbol{y} = g \cdot \boldsymbol{x} + \boldsymbol{n}_\Gamma$. A similar procedure as in the static channel is then performed to obtain the ergodic achievable rate. It can be seen from Figs. 3 and 4 that while there is a small gap between the proposed calculation and the Monte Carlo simulation when $\epsilon = 0.1$, the two results are almost identical when $\epsilon = 0.01$ at any values of Γ and p. Via extensive simulation results, we observe that $\epsilon = 0.01$ is sufficient to provide an accurate estimation of C_f. The proposed calculation can therefore serve as an attractive solution to calculate the rates.

5.3 Outage probability and capacity

In Fig. 5, the outage probability is plotted versus the achievable rate r using the calculation in (37) for $p = 0.1$, 0.2, and 0.5. Here, the error tolerance is chosen at $\epsilon = 0.01$. In line with the previous results, it can be observed from Fig. 5 that the derived outage probability fits very well with the Monte Carlo simulations. In this case, Monte Carlo simulations are performed by first calculating $r + h(\boldsymbol{n}_\Gamma)$ for a given r using 10^7 samples of the total noise plus interference. The outage probability can then be estimated by counting the number of samples $h(\boldsymbol{y}|g)$ that is smaller than $r + h(\boldsymbol{n}_\Gamma)$ and dividing by 10^7.

Similar results can also be seen with the alternative measure, the outage capacity. In particular, shown in Fig. 6 are the outage capacities against Γ when the systems are in 1, 5, and 10% outage. It is clear that the proposed calculation is in full agreement with the Monte Carlo simulations at the error tolerance $\epsilon = 0.01$.

6 Conclusion

In this paper, we proposed a simple and accurate method to calculate the achievable rates and outage probability of a CR link using DFH under a realistic condition of imperfect spectrum sensing for both static and Rayleigh fading channels. Specifically, over a static channel where the channel gain is assumed to be constant, we showed that the achievable rate of the considered CR link can be calculated using a simple series representation. The error introduced from the truncation of this representation is controllable. The calculation of the ergodic achievable rate in fast fading and the outage probability in slow fading was also studied. In particular,

IET Commun., 2015, Vol. 9, Iss. 17, pp. 2160–2167

based on the closed-form expression of the differential entropies calculated for the static channel, we introduced a PLCF-based method to approximate the instantaneous achievable rate curve. It was then demonstrated that the average achievable rate can be calculated effectively to achieve any given accuracy level. The PLCF-based method was also applied to effectively calculate the outage probability. Numerical results were finally provided to demonstrate the accuracy of the proposed methods.

Finally, it is worth mentioning that while we are able to provide effective numerical methods to calculate the achievable rates and outage probabilities, the proposed analytical results do not provide an insight on the behaviour of the considered CR systems. It is therefore very interesting to asymptotically study the effect of imperfect spectrum sensing to the performance of the CR systems under consideration. This interesting problem is currently under investigation.

7 References

1 Le, A.D., Tran, N.H., Duong, T.Q., *et al.*: 'Numerical calculation of achievable rates for cognitive radio with dynamic frequency hopping under imperfect spectrum sensing'. Proc. IEEE Int. Conf. on Communications and Electronics (ICCE), 2014, pp. 1–6

2 Goldsmith, A., Jafar, S., Maric, I., *et al.*: 'Breaking spectrum gridlock with cognitive radios: an information theoretic perspective', *Proc. IEEE*, 2009, **97**, (5), pp. 894–914

3 Willkomm, D., Gross, J., Wolisz, A.: 'Reliable link maintenance in cognitive radio systems'. Proc. of New Frontiers in Dynamic Spectrum Access Networks (DySPAN), 2005, pp. 371–378

4 Hu, W., Willkomm, D., Abusubaih, M., *et al.*: 'Cognitive radios for dynamic spectrum access – dynamic frequency hopping communities for efficient IEEE 802.22 operation', *IEEE Commun. Mag.*, 2007, **45**, (5), pp. 80–87

5 Wang, B., Liu, K.: 'Advances in cognitive radio networks: a survey', *IEEE J. Sel. Top. Signal Process.*, 2011, **5**, (1), pp. 5–23

6 Tandra, R., Sahai, A.: 'SNR walls for signal detection', *IEEE J. Sel. Areas Commun.*, 2008, **2**, pp. 4–17

7 Rao, A., Alouini, M.-S.: 'Performance of cooperative spectrum sensing over non-identical fading environments', *IEEE Trans. Commun.*, 2011, **59**, pp. 3249–3253

8 Tang, L., Chen, Y., Hines, E., *et al.*: 'Effect of primary user traffic on sensing-throughput tradeoff for cognitive radios', *IEEE Trans. Wirel. Commun.*, 2011, **10**, (4), pp. 1063–1068

9 Zhang, S., Zhao, H., Wang, S., *et al.*: 'A cross-layer rethink on the sensing-throughput tradeoff for cognitive radio networks', *IEEE Commun. Lett.*, 2014, **18**, (7), pp. 1226–1229

10 Li, S., Zheng, Z., Ekici, E., *et al.*: 'Maximizing system throughput by cooperative sensing in cognitive radio networks', *IEEE/ACM Trans. Netw.*, 2014, **22**, (4), pp. 1245–1256

11 Sharma, H., Patel, A., Merchant, S.N., *et al.*: 'Optimal spectrum sensing for cognitive radio with imperfect detector'. Proc. IEEE Vehicular Technology Conf. (VTC), 2014, pp. 1–5

12 Chen, Y., Yu, G., Zhang, Z., *et al.*: 'On cognitive radio networks with opportunistic power control strategies in fading channels', *IEEE Trans. Wirel. Commun.*, 2008, **7**, (7), pp. 2752–2761

13 Hanif, M.F., Smith, P.J.: 'On the statistics of cognitive radio capacity in shadowing and fast fading environments', *IEEE Trans. Wirel. Commun.*, 2010, **9**, (2), pp. 844–852

14 Zhang, J., Zheng, F., Gao, X., *et al.*: 'Sensing-energy efficiency tradeoff for cognitive radio networks', *IET Commun.*, 2014, **8**, (18), pp. 3414–3423

15 Ozcan, S.G.G., Gursoy, M.C.: 'Error rate analysis of cognitive radio transmissions with imperfect channel sensing', *IEEE Trans. Wirel. Commun.*, 2014, **13**, (3), pp. 1462–1655

16 Herath, S.P., Tran, N.H., Le-Ngoc, T.: 'Capacity limit of cognitive radio with dynamic frequency hopping under imperfect spectrum sensing'. IEEE Int. Symp. on Personal Indoor and Mobile Radio Communications (PIMRC), 2012, pp. 1693–1698

17 Khalid, L., Anpalagan, A.: 'Performance of cooperative spectrum sensing with correlated cognitive users' decisions'. Proc. IEEE Int. Symp. on Personal Indoor and Mobile Radio Communications (PIMRC), 2011, pp. 635–639

18 Kim, J., Shin, Y., Ban, T.W., *et al.*: 'Effect of spectrum sensing reliability on the capacity of multiuser uplink cognitive radio systems', *IEEE Trans. Veh. Technol.*, 2011, **60**, (9), pp. 4349–4362

19 Kaligineedi, P., Khabbazian, M., Bhargava, V.K.: 'Malicious user detection in a cognitive radio cooperative sensing system', *IEEE Trans. Wirel. Commun.*, 2010, **9**, (8), pp. 2488–2497

20 Stevenson, C., Chouinard, G., Lei, Z., *et al.*: 'IEEE 802.22: the first cognitive radio wireless regional area network standard', *IEEE Commun. Mag.*, 2009, **47**, (1), pp. 130–138

21 Cheng, W., Zhang, X., Zhang, H.: 'Full duplex spectrum sensing in non-time-slotted cognitive radio networks'. Proc. Military Communications Conf. (MILCOM), 2011, pp. 1029–1034

22 Vu, H.V., Tran, N.H., Nguyen, T.V., *et al.*: 'Estimating Shannon and constrained capacities of Bernoulli–Gaussian impulsive noise channels in Rayleigh fading', *IEEE Trans. Commun.*, 2014, **62**, (6), pp. 1845–1856

23 Gradshteyn, I.S., Ryzhik, I.M.: 'Table of integrals, series, and products' (Academic Press, Inc., 2000, 6th edn.)

24 Tse, D., Viswanath, P.: 'Fundamentals of wireless communication' (Cambridge University Press, New York, NY, USA, 2005)

8 Appendix 1: truncation of I_1

When the first $N-1$ terms of the series in I_1 are truncated, the error will be

$$\text{error} = \frac{1}{\beta_1}\sum_{n=N}^{\infty}\sum_{k=0}^{n}\binom{n}{k}\frac{(-1)^k x^{n+1}}{k+\mu+1} \tag{39}$$

Since $(1-v)^n < 1$, we have

$$x^{n+1}\int_0^1 v^{\mu}(1-v)^n\,\mathrm{d}v < x^{n+1}\int_0^1 v^{\mu}\,\mathrm{d}v. \tag{40}$$

It then follows that

$$\sum_{k=0}^{n}\binom{n}{k}\frac{(-1)^k x^{n+1}}{k+\mu+1} < \frac{x^{n+1}}{\mu+1} \tag{41}$$

Hence, the error will be upper-bounded as

$$\text{error} < \frac{1}{\beta_1}\sum_{n=N}^{\infty}\frac{x^{n+1}}{\mu+1} = \frac{1}{\beta_1(\mu+1)}\left(\frac{x^{N+1}}{1-x}\right). \tag{42}$$